

**CERN – European Organization for Nuclear Research**  
European Laboratory for Particle Physics



**CTF3 Note 048 (Tech.)**

**(Laser Amplifier, Photo-  
injector)**

**A HIGH PERFORMANCE DIODE-PUMPED Nd:YLF AMPLIFIER**

I.N. Ross, M. Csatári, S. Hutchins

**Abstract**

We report on the performance of a multi-pass diode-pumped amplifier designed to provide a combination of high gain and efficiency with high stability. A simple rod-cavity design and the establishment of quasi-steady-state operation resulted in a saturated gain of over 6000 at an average output intensity during the pulse train of  $7\text{kW}/\text{cm}^2$ . The amplifier showed an output stability of 0.2% rms in the short term and 0.7%rms in the long term, and an output intensity insensitive to input power changes. Zernike analysis of the measurements of pump distortion showed an almost pure astigmatic phase error which can be compensated up to high average power levels.

Geneva, Switzerland  
1 July 2002

# **A high performance diode-pumped Nd:YLF amplifier**

**Ian N.Ross**

*Central Laser Facility, Rutherford Appleton Laboratory,  
Chilton, Didcot, Oxon OX11 0QX, United Kingdom*

**Marta Csatári**

*Department of Optics and Quantum Electronics, University of Szeged,  
P.O.Box 406, Szeged 6701, Hungary*

**Steve Hutchins**

*PS Division, CERN, CH-1211 Geneve 23, Switzerland*

## **Abstract**

We report on the performance of a multi-pass diode-pumped amplifier designed to provide a combination of high gain and efficiency with high stability. A simple rod-cavity design and the establishment of quasi-steady-state operation resulted in a saturated gain of over 6000 at an average output intensity during the pulse train of  $7\text{kW}/\text{cm}^2$ . The amplifier showed an output stability of 0.2% rms in the short term and 0.7%rms in the long term, and an output intensity insensitive to input power changes. Zernike analysis of the measurements of pump distortion showed an almost pure astigmatic phase error which can be compensated up to high average power levels.

**OCIS codes:** (140.3280), (140.3480), (140.3580), (140.6810) Lasers and laser optics

## **A high performance diode-pumped Nd:YLF amplifier**

### **Introduction**

Potential applications of high average power lasers have led to intense research and development of diode-pumped systems. It is now possible to purchase a variety of such lasers, mainly directed towards engineering applications, but as yet these are unable to satisfy the many and often more difficult requirements of scientific applications. The work reported here is specifically directed towards meeting the requirements of one such application, to use a photo-cathode to generate the electron bunches suitable for injection into linear accelerators. Table 1. indicates the principle performance specification for a photo-injector laser to provide the electron bunch trains for the proposed future TeV linear accelerator, CLIC, at CERN. Such a laser would also provide the basis of suitable designs for a number of similar requirements in both particle physics and other areas.

Given the specification shown in Table 1. the basis of the laser system has been chosen to be a diode-pumped Master Oscillator-Power Amplifier laser operating at a wavelength of about 1  $\mu\text{m}$  and followed by a pair of non-linear crystals for conversion to a UV wavelength suitable for the photo-cathode. If a cw mode-locked oscillator is used, then this system offers the best opportunity for high stability and efficiency, and makes use of well proven diode pumping technology. The particular combination of requirements, for sub-10ps pulses, high gain and efficiency and low pump-induced distortion, led to the choice of Nd:YLF as the laser medium, although its low fracture stress would ultimately restrict the maximum average operating power.

Figure 1 illustrates the basic design of the photo-injector laser. A high average power cw mode-locked Nd:YLF laser operating at 500MHz serves as the oscillator. Since systems with pulse duration below 10ps, with powers of tens of watts and with mode-locked frequency up to

2GHz have been demonstrated<sup>1-4</sup> there is no need for further development and suitable systems are available commercially. The oscillator pulses are amplified and frequency converted to the fourth harmonic before relaying to the photo-cathode of the accelerator. Additional components in the laser system are likely to include feedback stabilisation, optics for beam relaying, spatial profile control, compensation for thermal distortion, and a Pockels' cell gate to define the ends of the pulse train.

The principal aspect of this laser system requiring development is the design and operation of the amplifiers. These must be efficient to minimise the cost of the pump diode arrays, have high gain to minimise the number of amplifiers and must show a very high degree of output stability. For cost and simplicity a cylindrical pumping cavity design is used as shown in Figure 2. Diode arrays are distributed around the rod using a geometry which ensures that (excluding reflection losses) at least 95% of the uncollimated diode output is intercepted by the rod. Residual unabsorbed pump radiation emerging from the back side of the rod is reflected back into the rod using coatings on the outside of the flow tube in regions not occupied by diode arrays. This ensures high absorption efficiency and helps to symmetrise the pump distribution over the rod cross-section. The rod is immersed in water both for cooling and to minimise reflection loss at the surfaces of rod (0.25%) and flow tube (0.2%). Such a design is best matched to a rod diameter of about 10mm but can work well for smaller rods if a simple lens is inserted in front of each diode array.

The average power limit of this amplifier using Nd:YLF is given by its fracture limit, of approximately 18W/cm, this being the maximum rate of deposition of heat per unit length of rod. Since the thermal dissipation into Nd:YLF due to the quantum defect is 32% of the excited state pump rate then it follows that the maximum extractable power is a factor  $(1-0.32)/0.32 = 2.13$

higher than the fracture limit, or 56W/cm. For example a 10cm rod could give a maximum output power of about 500W. Techniques to increase the fracture limit, such as that used for Nd:YAG<sup>5</sup>, may enable this limit to be extended.

The mode of operation of the amplifier must be selected so as to give a high gain but at the same time it is necessary to operate under conditions of heavy gain saturation in order to achieve high efficiency and stabilise the output power. We used a four pass geometry as shown in Figure 3. However for such a high gain system it will be important to establish the gain limit set by pump depletion resulting from amplified spontaneous emission. Such a limit could be a serious problem if too many passes are used with too close an optical coupling between passes.

In order to establish the best operating mode and optimise the performance a multi-pass analysis of this amplifier was carried out.

## **Analysis**

The analysis is given for Nd:YLF but can readily be used for other materials and amplifier designs. The examples used will be for the test amplifier as used for all the experimental results given below. This amplifier is fitted with a 5mm diameter by 50mm long rod of Nd:YLF and is pumped by 5 stacked diode arrays each providing a peak pump power of 1kW. The diode arrays are QCW and can be operated at up to 2% duty cycle. Most of the test data was taken at 5Hz with a square pump pulse of duration up to 800 $\mu$ s.

The amplifier is most stable when it is operated in a 'quasi-steady-state' mode. If this can be established during the pump time then the excited state population levels in the amplifier do not change with time and there will be a balance between the input pump power reaching the

upper laser level (pump rate) and the sum of the power lost to the amplified beam and to amplified spontaneous emission (ASE), or:

$$I_p = I_{out} - I_{in} + \frac{F_{sat} \cdot \ln G}{\eta_R} \frac{1 + B}{\tau_{fl}} \quad (1)$$

where:  $I_p, I_{out}, I_{in}$  are the pump rate, output intensity and input intensity respectively

$F_{sat}$  = saturation fluence;       $G$  = amplifier gain

$\eta_R$  = splitting ratio in the upper laser level

$\tau_{fl}$  = fluorescence lifetime of the excited state

and where  $B$  is the increase in the excited state decay rate resulting from ASE.

Since the contribution to the intensity ( $dI_p$ ) at any position P in the rod from a volume element  $dV$  at a distance  $r$  can be written  $f(N/\tau)h\nu \exp[\alpha r]dVd\Omega = (f\alpha I_{sat} \exp[\alpha r]dV)/4\pi r^2$ , and since this leads to a rate of change of excited state population at P given by  $(N/\tau)(dI_p/I_{sat})$  the value of  $B_p$  can be calculated from:

$$B_p = f\alpha \int_{rod} \frac{\exp(\alpha r)}{4\pi r^2} dV \quad (2)$$

where:  $f$  = fraction of excited state population fluorescing at the laser wavelength

$\alpha$  = gain coefficient

and the integral is evaluated over the volume V of the rod and must include surface reflections.

Equations 1 and 2 need to be reformulated to apply to our 4-pass test amplifier. Assuming a constant beam size from pass to pass and an intra-pass loss of L, equation 1 can be re-written as:

$$I_p = f_1(G)I_{in} + f_2(G) \quad (3)$$

Where:

$$f_1(G) = (1-L)^3 G^4 + (1-L)^2 LG^3 + (1-L)LG^2 + LG - 1 \quad \text{and} \quad f_2(G) = \frac{F_{sat} \ln G (1+B)}{\eta_R \tau_{fl}}$$

and where:  $G$  = single pass gain of amplifier

For a 4-pass amplifier with good decoupling (for example a long distance) between passes and for a rod with a diffuse barrel surface, an approximate expression for  $B$  is:

$$B = 0.05(d/l)^{0.3} G \quad (4)$$

for a rod of length  $l$  and diameter  $d$ .

In this analysis since the pulse trains in question have an individual pulse fluence very small compared to the saturation fluence, the gain characteristics of the amplifier are not dependent on the pulse nature of the beam and valid results can be obtained by assuming the input beam to be continuous.

The extraction efficiency ( $\eta_{ex}$ ) of the amplifier, is defined here as the ratio of the intensity increase of the amplified beam to the pump rate:

$$\eta_{ex} = \frac{I_{out} - I_{in}}{I_p} \quad (5)$$

Since the ASE loss increases with gain, there will necessarily be a compromise between efficiency and gain. For our 4-pass test amplifier Figure 4 shows the calculated variation of efficiency with 4-pass gain and predicts that gains of more than  $10^4$  can be obtained with Nd:YLF without a major reduction in efficiency.

Two measures of stability can be derived for steady state operation by differentiating equation 1 to give:

$$dI_p = (f_1' I_{in} + f_2') dG + f_1 dI_{in} \quad (6)$$

Use of the substitution  $I_{out} = (1-L)^3 \cdot G^4 \cdot I_{in}$  leads to an equation for the interdependence between changes in input, pump and output intensities:

$$I_p \frac{dI_p}{I_p} = \frac{G}{4} (f_2' + f_1' I_{in}) \frac{dI_{out}}{I_{out}} - \left[ \frac{G}{4} (f_2' + f_1' I_{in}) - f_1 I_{in} \right] \frac{dI_{in}}{I_{in}} \quad (7)$$

where  $f_1', f_2'$  are the differentials of  $f_1$  and  $f_2$  respectively with respect to  $G$ . For the test amplifier with measured values of 9 for  $G$ ,  $4.7 \text{ kW/cm}^2$  for  $I_{out}$ , and 0.2 for  $L$  this reduces to:

$$\frac{dI_{out}}{I_{out}} = 1.85 \frac{dI_p}{I_p} + 0.163 \frac{dI_{in}}{I_{in}} \quad (8)$$

The stability for the laser system is consequently largely determined by the stability of the pumping rate of the final amplifier and can support much larger variations from earlier in the system.

Having established the expected performance in the steady state mode it is useful to consider the process by which the steady state can be reached. To do this we calculate the dynamic response of the amplifier in the presence of a time-varying pump and input signal beam. The dynamics of the amplifier are described by the spatial and temporal changes to the amplifier gain coefficient. For an input pulse train with a time separation of  $\tau_s$  between pulses the incremental change in the gain coefficient from one pulse to the next has three contributions: the increase due to pumping; the loss due to fluorescence enhanced by amplified spontaneous emission; and the depletion by the previous pulse. The net change is given by:

$$\Delta\alpha(z, t) = \frac{\eta_R}{F_{sat}} \frac{I_p(z, t) \tau_s}{l} - \frac{\alpha(z, t) \tau_s (1 + B)}{\tau_{fl}} - \frac{\alpha(z, t) \eta_R F(z, t)}{F_{sat}} \quad (9)$$

where:  $\eta_R$  = level splitting ratio in the upper laser state and it is assumed that the

equilibrium in the level populations is re-established in a time short compared with  $\tau_s$ .

$F(z, t)$  = the sum of the pulse fluences in all passes at position  $z$  and time  $t$ .

For a single pass amplifier the pulse fluence at  $(z, t)$  is given by:

$$F(z, t) = F_{in} \exp \int_0^z \alpha(z, t) dz \quad (10)$$

and for a 4-pass amplifier it is given by:

$$F(z, t) = F_{in}(t) \left[ \begin{array}{l} \exp \int_0^z \alpha(z, t) dz + L \exp \left( \int_0^l \alpha(z, t) dz + \int_z^l \alpha(z, t) dz \right) \\ + L^2 \exp \left( 2 \int_0^l \alpha(z, t) dz + \int_0^z \alpha(z, t) dz \right) + L^3 \exp \left( 3 \int_0^l \alpha(z, t) dz + \int_z^l \alpha(z, t) dz \right) \end{array} \right] \quad (11)$$

Solving these equations for the test 4-pass amplifier with a constant fluence input pulse train of average power 500mW, and a constant pump pulse starting at  $t = 0$ , gives the output fluence shown in Figure 5. It can be seen that steady-state operation is achieved after 500 $\mu$ s with a perfectly stable output after this time. Such a mode of operation of the amplifier suffers from an additional efficiency loss during the build-up time of the output pulse fluence. This can be reduced by gating the input pulse train to turn on some time after initiation of the pump at a time when the gain has first reached its steady-state value<sup>6</sup>. In this case the pre-pump period, during which the output efficiency is zero, is reduced to 300 $\mu$ s. However the timing accuracy of the input gate must be better than  $\sim 20\mu$ s in this case and leads to an additional and perhaps unnecessary complexity to the system.

### **Test amplifier performance**

An amplifier head was constructed to the design shown in Figure 2 and used to pump a 5mm diameter by 50mm long rod of Nd:YLF. 5 QCW 1kW stacked diode arrays (Thales) were distributed around the rod as shown in Figure 2 and an additional lens in front of each array

ensured efficient optical coupling to the rod. The diode wavelengths were in the range 798 to 802 nm to provide good absorption efficiency for both polarisations<sup>7</sup> Repetition rate was normally 5Hz with pump duration in the range 400 - 800 $\mu$ s.

The input seed beam was provided by an 800mW CW Nd:YLF laser (Crystalaser) and the injection optics of the 4-pass geometry gave a beam size of 4mm in the first pass and adjustable down to 1mm in the final pass. The propagation distance between passes of 1m ensured low ASE pass-to-pass coupling and good beam overlap in all passes.

### Gain and saturation

Figure 6 shows the fluorescence distribution in the rod for pumping with individual diode arrays and with all five arrays together. The effect of pump polarisation is seen since the top diode polarisation at the rod is 's' which is more strongly absorbed by the rod, and the bottom diodes are mostly 'p' polarisation at the rod and the absorption is less. The combined effect of all diodes is equivalent to 50% 's' and 50% 'p' and provides quite uniform pumping as illustrated in the centre image showing the heavily saturated gain distribution.

The ability of the amplifier to generate high gain is shown in Figure 7 by the measured evolution of the small signal gain during the 600 $\mu$ s pump duration. Also shown is a calculated profile for which the best match to the measured curve gave a combined pump cavity transfer and rod absorption efficiency of 53%. The peak gain achieved was  $5 \times 10^5$  with a background ASE intensity measured at the  $10^{-3}$  level.

At the maximum available input power into the first pass of 450mW it was possible to strongly saturate the amplifier, giving the evolution of output intensity shown in Figure 8. This is seen to be in good agreement with the calculated profile, and in this case the steady state is

reached after 350 $\mu$ s as expected, with an output intensity at 7kW/cm<sup>2</sup> which is 8x the saturation intensity for Nd:YLF.

Further evidence for the degree of saturation is indicated by the change in output beam spatial profile as a result of the amplification (Figure 9). This amplified beam has a flat-top of diameter 2.5mm containing a peak power of 380W, in comparison with the unamplified approximately Gaussian profile with FWHM of 1mm.

### Stability

The output pulse train stability is a critical feature of this type of laser system as indicated by the required specification in Table 1 and this must be maintainable over periods of perhaps several hours. The proposed design of system aims to achieve the best possible stability by using diode pumping and by relying on heavy saturation of the amplifiers to provide a strong clamp on the output intensity. As indicated by the earlier 'steady-state' analysis such a design largely confines the problem to stabilising the pump rate in the final amplifier. This is dependent on two principal factors: the current to the diode array, and the temperature of the coolant, the latter having a strong influence on the diode spectrum and hence the absorption efficiency of the laser rod. In our system the diode driver was stable to about 0.5% long term and the temperature of the coolant was maintained to 0.5deg. Evidently both of these could be improved. An indication of the need for precise control of temperature is shown by an example of the measured variation of output with temperature shown in Figure 10.

Stability measurements were conducted using an InGaAs photodiode which has a very low temperature coefficient at 1047nm and is not sensitive to background visible radiation, together with an oscilloscope with stability in the region of 0.1%. Allowing a period of at least 30 minutes for stabilisation, the short and long term stability of the output power was measured

and is shown in Figure 11. The rms stability was measured at less than 0.2% in short term and less than 0.7% over a period of one hour. This excellent performance was achieved without special precautions to stabilise the mechanics and environment and without any feedback stabilisation system. In order to demonstrate the insensitivity to variations of the amplifier input power the amplifier was operated at maximum gain saturation (top curve in figure 12) and the oscillator was then attenuated by a factor  $\sim 10$ . This led to a reduction of only a few % in the saturated output of the amplifier (middle curve of Figure 12).

#### Thermal aberrations in the amplifier

In the photo-injector application under consideration, and in many others, the optical integrity of the amplified beam is important and one good reason for selecting Nd:YLF as the gain medium is its much reduced thermal lensing in comparison with other materials such as Nd:YAG<sup>8</sup>. A radial shear Sagnac interferometer placed in the amplified beam was used to assess the thermal lensing, and the recorded interferograms were analysed using a CCD, frame store and software package (OFA). Examples of the interferograms recorded with and without amplifier pumping and for orthogonal orientations are shown in Figure 13 for 10 watts average thermal power deposited in the rod. A Zernike analysis of these interferograms yielded significant coefficients only for primary astigmatism and defocus, indicating that the aberration can be effectively compensated using cylindrical lenses. Using the measured Zernike coefficients, the Strehl ratio was calculated and plotted in Figure 14 with an extrapolation to higher powers. For example, taking 0.8 as a minimum acceptable value for the Strehl ratio, this analysis predicts that the amplifier can be used up to a thermal power of 15 W without requiring optical compensation and this corresponds to an output average power of up to 40 W for an amplifier operating at high efficiency. A further factor of 6 increase in output power is possible

with this amplifier before reaching the fracture point of the rod, but at these levels astigmatic compensation would be required.

## **Conclusion**

We have proposed and analysed a 'quasi-steady-state' mode of operation for a pulsed diode-pumped laser amplifier. Under heavy saturation this amplifier has high extraction efficiency and is highly stable being only sensitive to changes in its diode pump power and temperature. In multi-pass operation the amplifier can also have high gain and be very insensitive to changes in input beam energy or power.

A simple design of amplifier capable of high power and based on Nd:YLF has been constructed and tested. Its performance provided good verification for the analytical predictions for gain and efficiency, and the optical quality of the amplifier at high average power was assessed. The most promising aspect of this amplifier has been the measured output pulse stability. At 0.7%rms over 1 hour this already competes favourably with the best previous measurements on lasers and we know this can be improved using a more stable diode-laser power supply and improved coolant temperature stabiliser. Additional stabilisation is also achievable using a closed cycle feedback control system.

## References

1. Y.Hirano, Y.Koyata, S.Yamamoto, K.Kasahara, T.Tajime "208-W TEM<sub>00</sub> operation of a diode-pumped Nd: YAG rod laser" Optics Letters **24**, 679-681, (1999)
2. T. H. Graf, A. I. Ferguson, E. Bente, D. Burns, M. D. Dawson "Multi-Watt Nd:YVO<sub>4</sub> laser, mode locked by a semiconductor saturable absorber mirror and side-pumped by a diode-laser bar" Opt. Comm. **159**, 84-87, (1999)
3. G. Cerullo, S. De Silvestri, V. Magni, "High efficiency, 40 W Nd:YLF laser with large TEM<sub>00</sub> mode," Opt. Comm. **17**, 77-81, (1992).
4. K.J.Weingarten, D.C.Shannon, R.W.Wallace, U.Keller "Two-gigahertz repetition-rate. diode-pumped, mode-locked Nd:YLF laser" Opt. Lett. **15**, 962-964, (1990)
5. J.Marion "Strengthened solid-state laser materials" Appl.Phys.Lett. **47**, 694-696, (1985)
6. I.Will, A.Liero, D.Mertins, W.Sandner "Feedback-Stabilized Nd:YLF Amplifier System for Generation of Picosecond Pulse Trains of an Exactly Rectangular Envelope" IEEE J.Q.E. **34**, 2020-2028, (1998)
7. N.P.Barnes, M.E.Storm, P.L.Cross, M.W.Skolaut, "Efficiency of Nd Laser Materials with Laser Diode Pumping", IEEE JQE **QE-26**, 558-568, (1990)
8. J.E.Murray "Pulsed Gain and Thermal Lensing of Nd:LiYF<sub>4</sub>" IEEE J.Q.E.**19**, 488-491, (1983)

## Figure Captions

- Figure 1 Basic design of the photo-injector laser system
- Figure 2 Schematic of the amplifier head
- Figure 3 a) The experimental arrangement for the diode-pumped amplifier system  
b) The four-pass amplifier geometry
- Figure 4 The variation of the efficiency of extraction of pump power with the amplifier gain
- Figure 5 The calculated amplified intensity during the pumping period.
- Figure 6 The fluorescence distribution across the rod due to the diode arrays individually and the saturated gain distribution with all diode arrays together.
- Figure 7 The calculated and measured small signal gain of the amplifier.
- Figure 8 The calculated and measured gain for the amplifier under strong saturation.
- Figure 9 Unamplified and amplified output beam distributions showing the effect of strong saturation, which generates a flat-top from a Gaussian profile.
- Figure 10 The dependence of the amplified signal for different coolant temperatures.
- Figure 11 Short-term and Long-term stability of the amplified signal with strong saturation.
- Figure 12 Low sensitivity of the amplified signal to a large attenuation of the input signal.
- Figure 13 Interferograms showing the thermal optical distortion of the amplifier for a heat deposition rate of 10 watts. a) and b) show the interferograms for orthogonal orientations without and with pumping respectively.
- Figure 14 The Strehl Ratio calculated from the measured optical distortions and extrapolated up to the fracture limit of the amplifier rod.

Table 1 Photo-cathode specifications for the CLIC photo-injector.

|                             |              |
|-----------------------------|--------------|
| <b>UV energy/pulse</b>      | 5 $\mu$ J    |
| <b>Pulse duration</b>       | 10 ps        |
| <b>Wavelength</b>           | <270 nm      |
| <b>Time between pulses</b>  | 2.13 ns      |
| <b>Pulse train duration</b> | 91.6 $\mu$ s |
| <b>Repetition rate</b>      | 100 Hz       |
| <b>Energy stability</b>     | <0.1%        |

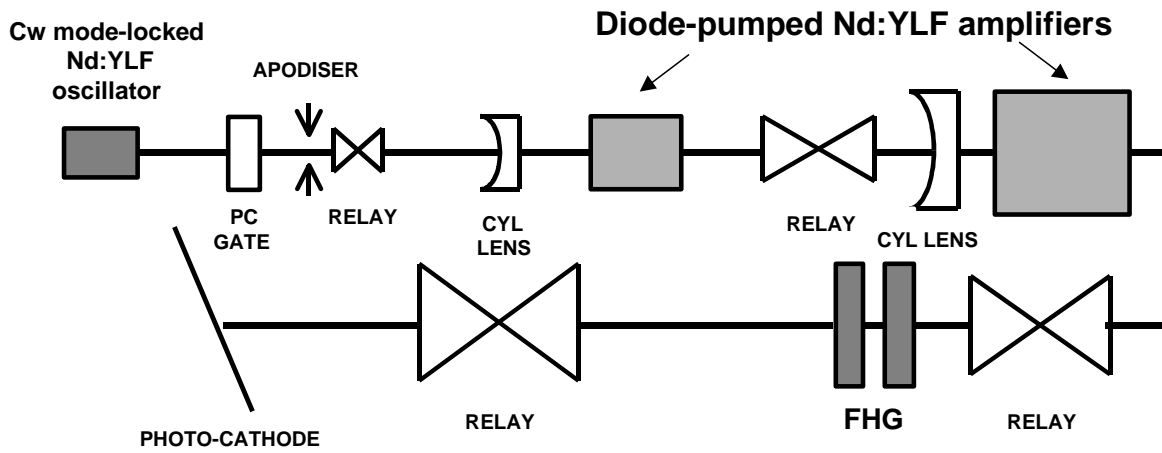


Figure 1 Basic design of the photo-injector laser system

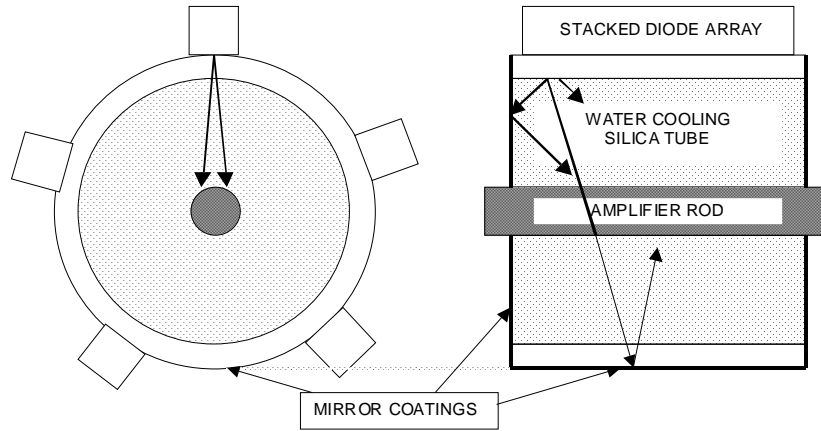
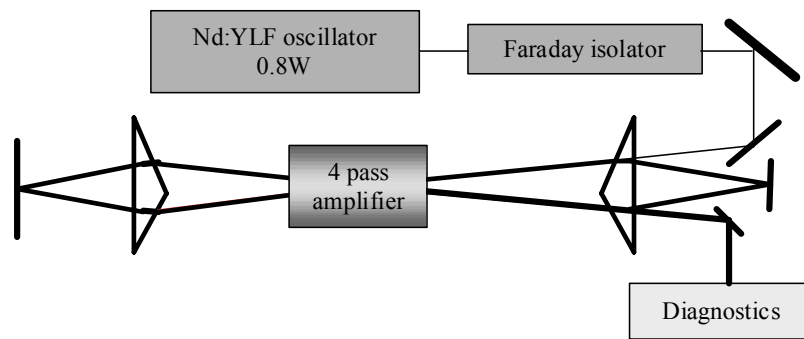
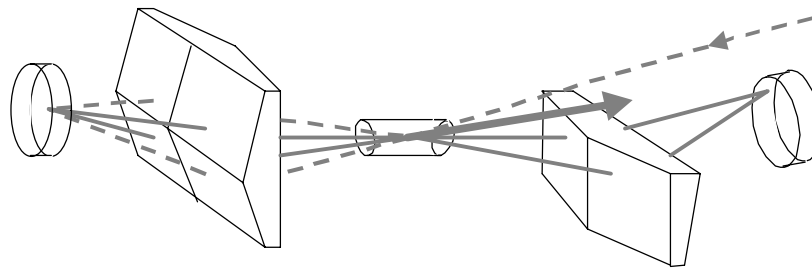


Figure 2 Schematic of the amplifier head



a)



b)

Figure 3 a) The experimental arrangement for the diode-pumped amplifier system  
b) The four-pass amplifier geometry

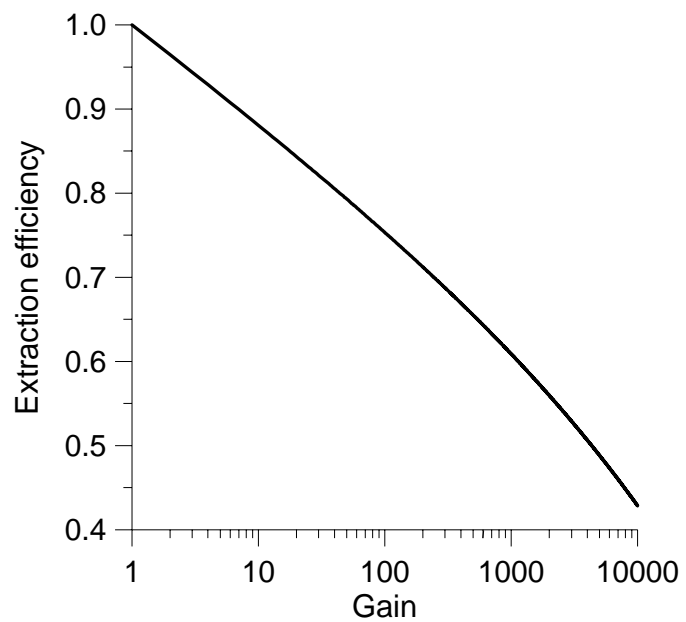


Figure 4 The variation of the efficiency of extraction of pump power with the amplifier gain

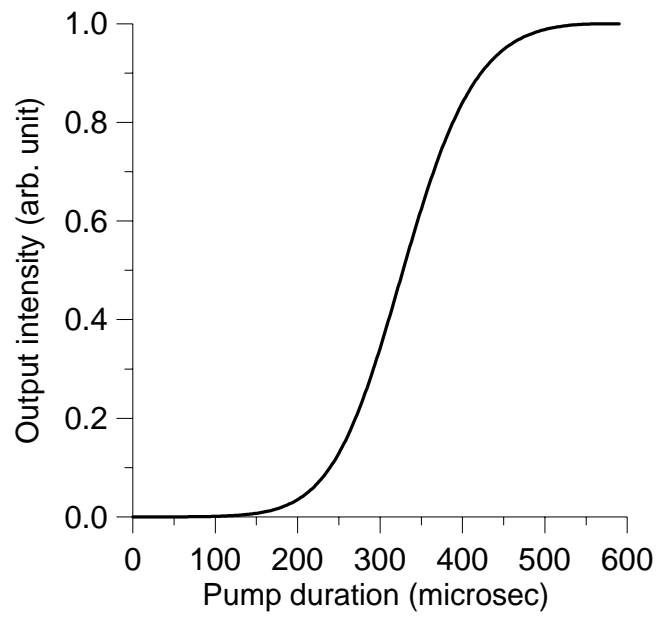


Figure 5 The calculated amplified intensity during the pumping period.

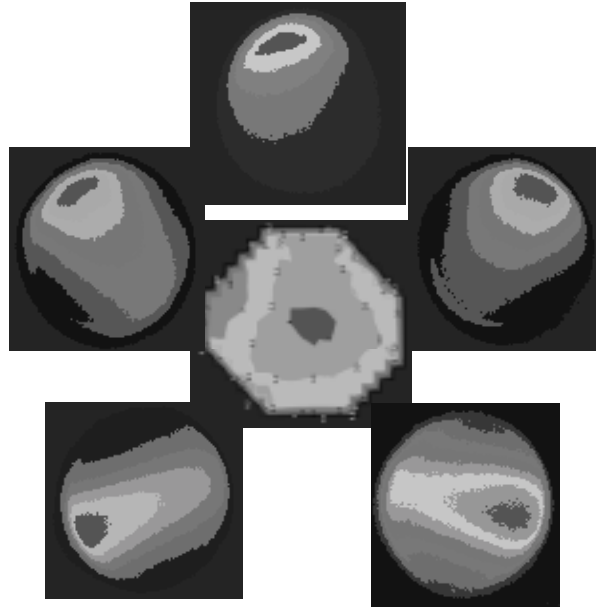


Figure 6 The fluorescence distribution across the rod due to the diode arrays individually and the saturated gain distribution with all diode arrays together.

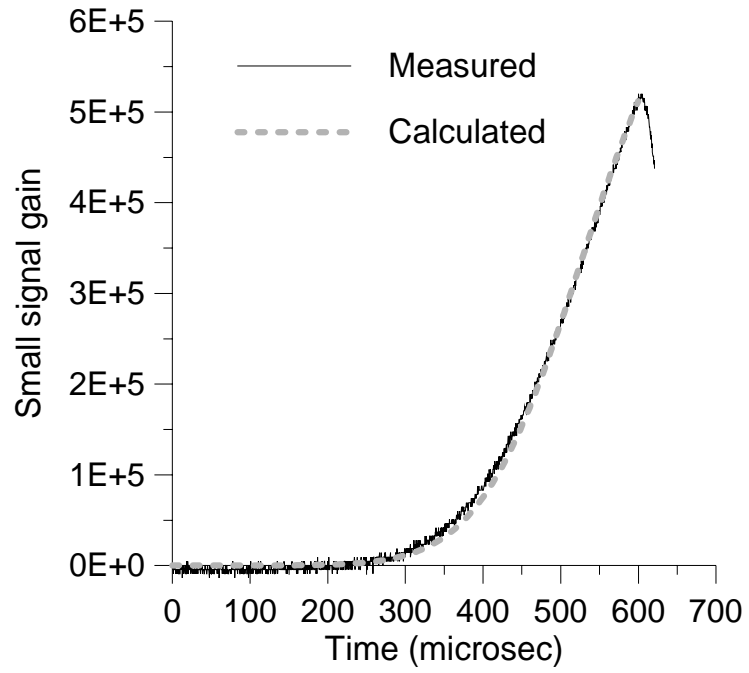


Figure 7 The calculated and measured small signal gain of the amplifier.

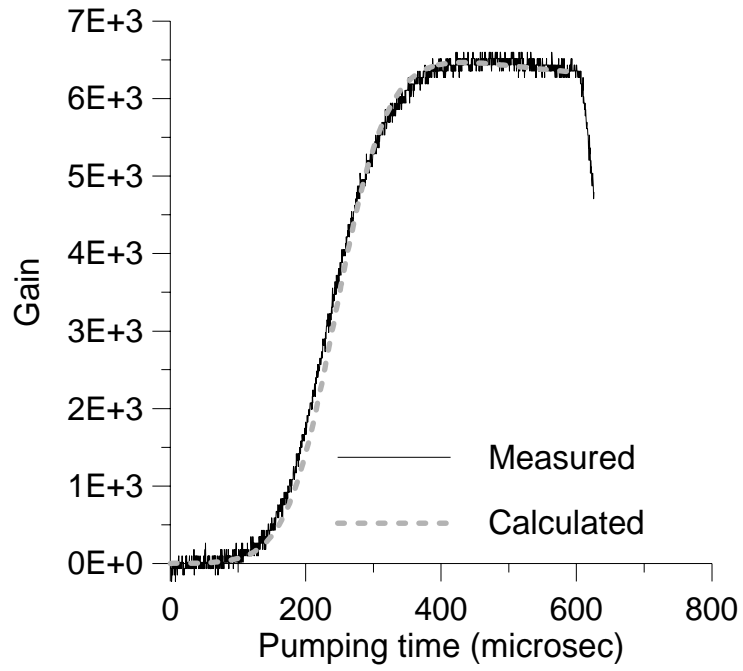


Figure 8 The calculated and measured gain for the amplifier under strong saturation.

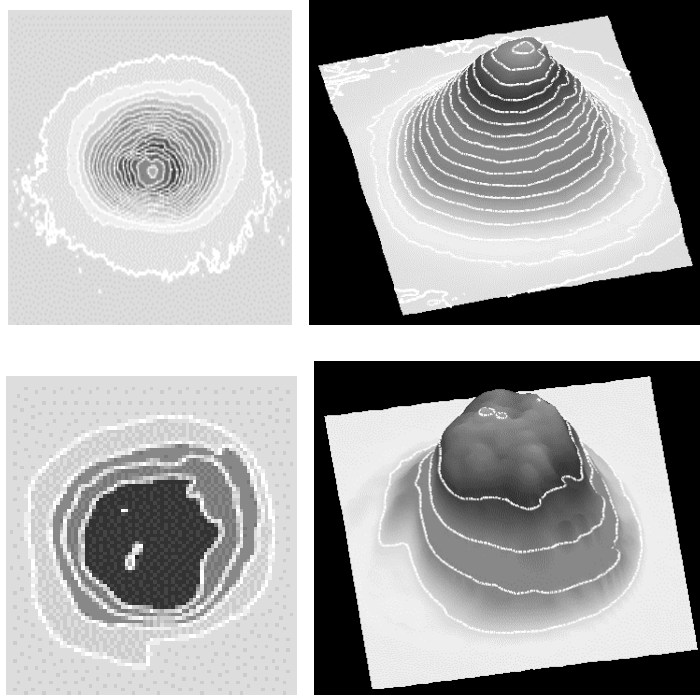


Figure 9 Unamplified (upper) and amplified (lower) output beam distributions showing the effects of strong saturation, which generates a flat-top from a Gaussian profile.

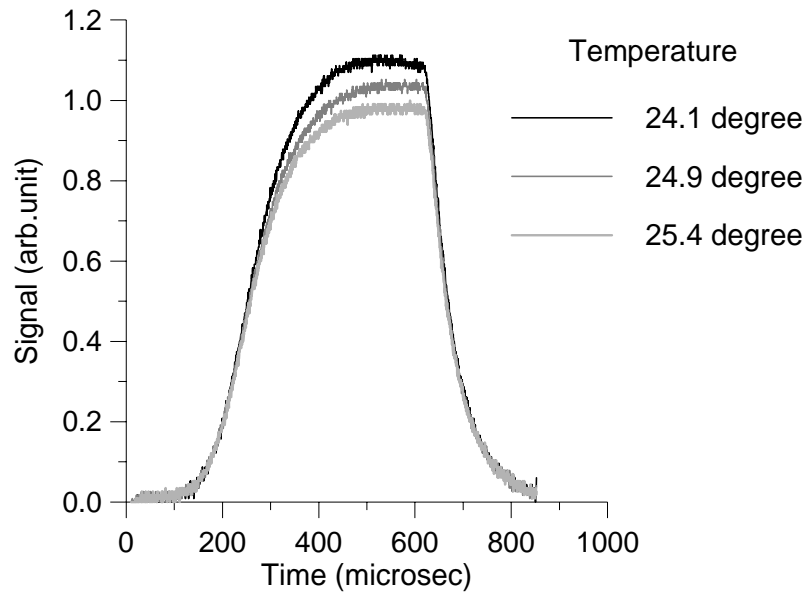


Figure 10 The dependence of the amplified signal for different coolant temperatures.

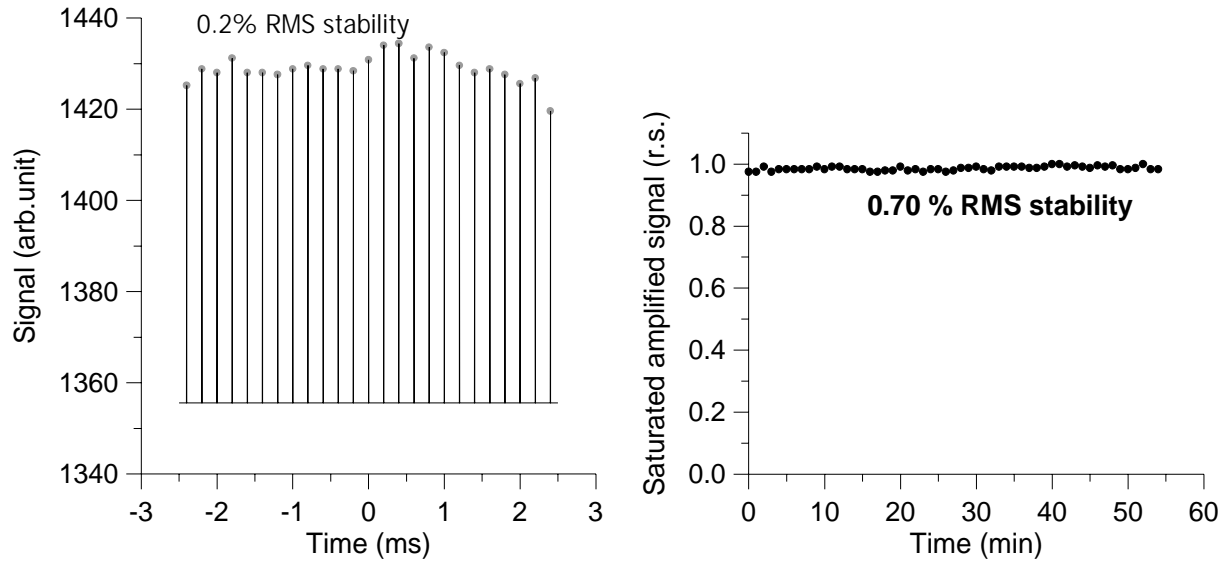


Figure 11 Short-term and Long-term stability of the amplified signal with strong saturation.

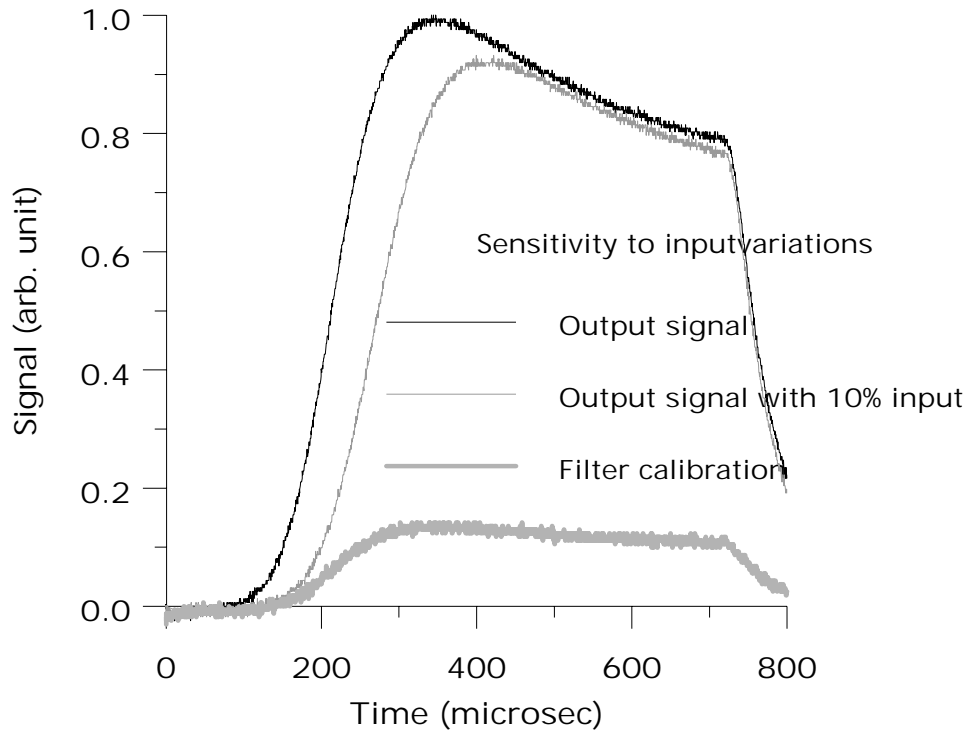


Figure 12 Low sensitivity of the amplified signal to a large attenuation of the input signal.

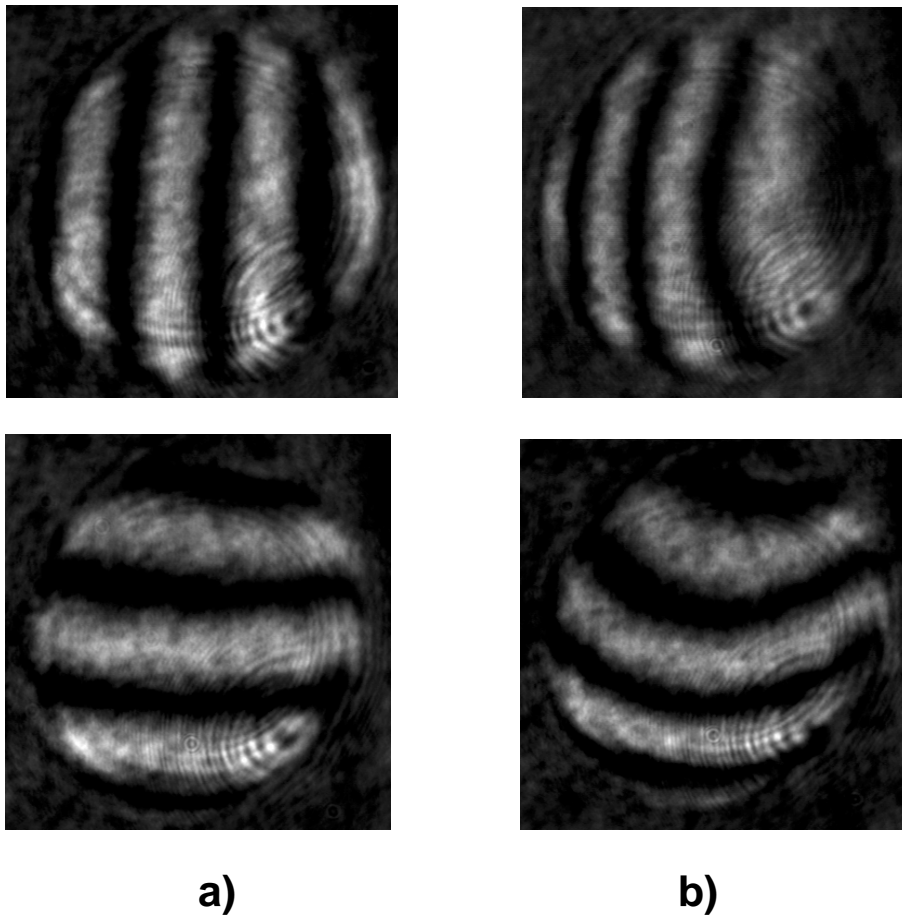


Figure 13 Interferograms showing the thermal optical distortion of the amplifier for a thermal deposition rate of 10 watts. a) and b) show the interferograms for orthogonal orientations without and with pumping respectively.

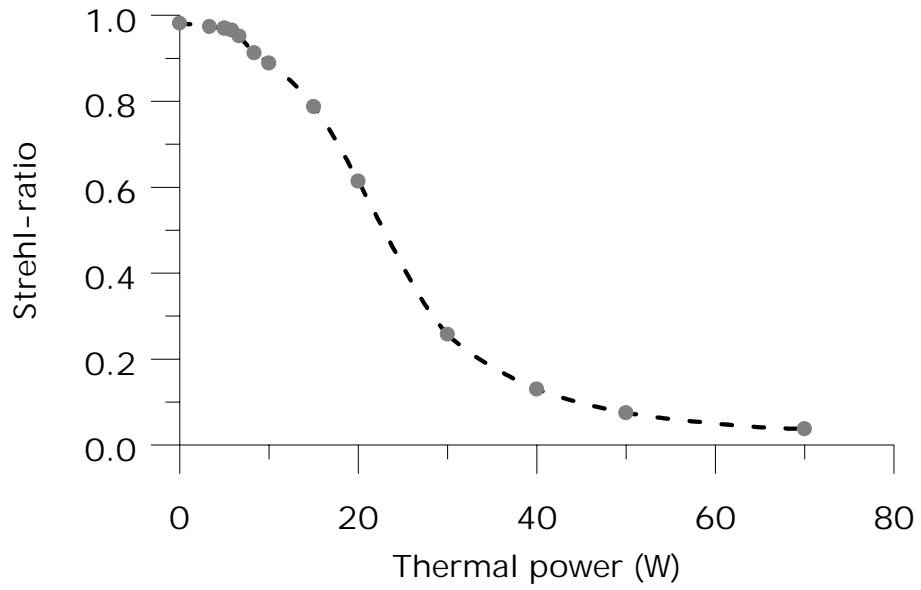


Figure 14 The Strehl Ratio calculated from the measured optical distortions and extrapolated up to the fracture limit of the amplifier rod.